

Accepted Manuscript

Geochemical speciation of mercury in bauxite

C. Staun, J. Vaughan, M.A. Lopez-Anton, M. Rumayor, M.R. Martínez-Tarazona

PII: S0883-2927(18)30065-9

DOI: [10.1016/j.apgeochem.2018.03.007](https://doi.org/10.1016/j.apgeochem.2018.03.007)

Reference: AG 4055

To appear in: *Applied Geochemistry*

Received Date: 3 April 2017

Revised Date: 5 February 2018

Accepted Date: 7 March 2018

Please cite this article as: Staun, C., Vaughan, J., Lopez-Anton, M.A., Rumayor, M., Martínez-Tarazona, M.R., Geochemical speciation of mercury in bauxite, *Applied Geochemistry* (2018), doi: [10.1016/j.apgeochem.2018.03.007](https://doi.org/10.1016/j.apgeochem.2018.03.007).

This is a PDF file of an unedited manuscript that has been accepted for publication. As a service to our customers we are providing this early version of the manuscript. The manuscript will undergo copyediting, typesetting, and review of the resulting proof before it is published in its final form. Please note that during the production process errors may be discovered which could affect the content, and all legal disclaimers that apply to the journal pertain.



1
2
3
4
5
6
7
8
9
10
11
12
13
14
15
16
17
18
19
20
21
22
23
24
25
26
27

Geochemical Speciation of Mercury in Bauxite

C. Staun^a, J. Vaughan^a, M.A. Lopez-Anton^b, M. Rumayor^b, M.R. Martínez-Tarazona^b

^aUniversity of Queensland Rio Tinto Bauxite & Alumina Technology Centre, St Lucia, 4072, Brisbane, Australia

^bInstituto Nacional del Carbón (CSIC), Francisco Pintado Fe, 26, 33011, Oviedo, Spain

*Corresponding author: Chris Staun

Email: c.staun@uq.edu.au

28 **Abstract**

29 The presence of trace concentrations of mercury in bauxite is a potential environmental concern in
30 the Bayer alumina refining process. An understanding of the geochemical speciation of mercury in
31 bauxite provides insight into the behaviour of mercury in the Bayer process. The speciation of
32 mercury was evaluated using a novel continuous thermal desorption methodology, sequential
33 extractions, alkaline digestion, aqua regia digestion and hydrofluoric acid total dissolution assay.
34 Thermal desorption demonstrated two distinct mercury forms. Labile mercury was found to be
35 present as metacinnabar or organic-associated mercury, while refractory mercury was associated
36 with quartz or other refractory silicates.

37

38 **Keywords:** mercury; bauxite; speciation; thermal desorption; sequential extraction

39

40

41

42

43

44

45

46

47

48

49

1. Introduction

The refining of alumina is performed using the Bayer process, which involves the alkaline digestion of bauxite ore in order to dissolve amphoteric aluminium hydroxides that leave a predominantly iron oxide residue. Lateritic bauxites are formed in tropical climates through the weathering and dissolution of parent silicates resulting in the precipitation of aluminium hydroxide in the form of gibbsite or boehmite. Mercury is present in bauxite in trace concentrations and due to its electrochemical nobility, hydrophobic character and volatility may deport to condensate waters, presenting problems of an environmental and safety management nature. Mercury is a bio-accumulative neurotoxin with a complex biogeochemical cycle and is subject to increasingly stringent regulation. It is within this framework that technologies have been developed for the remediation of Bayer process stack emissions and condensates (Mullett et al., 2012, Mullett et al., 2007).

The University of Queensland - Rio Tinto Bauxite and Alumina Technology Centre has evaluated the chemical thermodynamics of mercury in the Bayer process and demonstrated the feasibility of techniques for stabilising mercury to a non-volatile phase in Bayer digestion, preventing the deportment of mercury to condensate (Bansal et al., 2014b, Staun et al., 2016). Robust analytical techniques have been developed for the determination of mercury in all Bayer materials (Bansal et al., 2014a). Identification of the geochemical speciation of mercury in bauxite will further contribute to an understanding of the behavior of mercury in the Bayer process, and potentially allow the development of novel process additives.

Determining mercury speciation in bauxite is not an easy task due to the diverse chemical associations of trace metals. Spectroscopic x-ray absorption methods are not useful in this instance, as mercury concentration is in the parts per billion range, below the limits of detection (Jew et al., 2011). However, thermal desorption methodology (HgTPD) for mercury speciation appears to be a new, promising analytical technique for identifying mercury species in solids. This technique

75 exploits the temperature-dependent sublimation of mercury compounds, an effective procedure for
76 the identification of mercury species at concentrations lower than 10 ppm (Rumayor et al., 2013,
77 Rumayor et al., 2015a). In the present work, HgTPD analysis was performed on different bauxite
78 samples and complimented by a series of sequential extractions, a widely used methodology in soil
79 science to determine geochemical speciation. The total mercury concentration was determined by
80 means of a hydrofluoric acid total dissolution assay, the results of which were in close correlation to
81 those of an alkaline digestion methodology. This work explores the geochemical speciation of
82 mercury in five lateritic bauxites using the above-mentioned methods.

83

84 2. Experimental

85

86 2.1. Sample preparation

87 A total of 5 lateritic bauxites were employed for this study. All of the bauxite samples were
88 milled to 100 % passing 150 μm with the exception of bauxite 5 (NIST 600). This is a standard
89 reference material supplied by the National Institute of Standards and Technology, milled to 80 μm .

90

91 2.2. Sequential extraction of mercury

92 Sequential extractions were completed as per the methodology of Bloom et al. (2003). A sub
93 sample of bauxite was sequentially extracted using solutions of increasing chemical reactivity. The
94 fractions in the order of 1 to 5 were deionised water, 0.1 M acetic acid and 0.01 M hydrochloric
95 acid, 1 M potassium hydroxide, 12 M nitric acid and finally *aqua regia*. The extractions were
96 performed at room temperature for 24 ± 2 hours. The vessels were attached to a barrel rotating
97 horizontally at 20 rpm with the exception of F5 which was left to stand for 24 hours in loosely
98 capped vials to prevent pressure build-up due to the generation of chlorine gas. The size of each
99 sample was 0.4 g, while the extractant volume was 40 mL, with the exception of F5 which was 13

100 mL. 5 replicates for each bauxite sample were used. The extractant solutions were analysed using a
101 Perkin Elmer flow injection mercury system (FIMS 400) to matrix-matched calibration standards,
102 as per the methodology of Bansal et al. (2014a). Each replicate was analysed 3 times and the mean
103 value was taken as the result. 95 % confidence intervals were generated using a two-tail Student`s
104 distribution (error bars).

105

106 2.3. Hydrofluoric acid total dissolution assay

107 Total mercury bauxite concentrations were determined using hydrofluoric acid-assisted
108 digestion in a Speedwave 4 microwave digestion unit. The bauxite solid loading was 0.4 g. The
109 total extractant volume was 20 mL: 10mL aqua regia, 5 mL hydrofluoric acid, 1.5 mL hydrogen
110 peroxide and 3.5 mL deionised water. 5 replicate digestions were performed for 60 minutes at 230
111 °C. This ensured the total dissolution of the bauxite matrix, leaving only a fine fluoride precipitate.

112

113 2.4. Aqua regia digestion

114 Aqua regia digestion was performed for the same temperature and duration as hydrofluoric
115 acid, with a solid loading of 1.5 g, and a solution composition of 3.75 mL HCl, 1.25 mL HNO₃, 1
116 mL H₂O₂ and 9 mL deionised water. The solution was analysed using a FIMS 400 to matrix-
117 matched calibration standards, with confidence intervals generated as per Section 2.2.

118

119 2.5. Alkaline digestion

120 The alkaline digestions were performed in a rotating pressurised digestion vessel, in imitation
121 of a low-temperature Bayer process. 5 replicate digestions were carried out for 1 hour at 140 °C
122 using an alumina refinery sourced digestion stage alkaline with 4 M free sodium hydroxide. 5 g of
123 bauxite was added to 25 mL of extractant, resulting in the complete dissolution of the gibbsite. The
124 post-digestion solution and solid residue was analysed using a Milestone DMA-80 thermal

125 desorption instrument, and the mercury concentration in the pre-digestion bauxite was determined
126 by means of a mass balance. The temperature was ramped to 750 °C and held at this temperature for
127 three minutes. Flocculation of the solid residue prior to filtration resulted in the formation of
128 insignificant concentrations of mercury in the filtrate. Confidence intervals were generated as per
129 Section 2.2, using a DMA-80. Each replicate was analysed 3 times. Detection limits were
130 determined using 10 replicates of blank solution as the standard deviation multiplied by 3.

131

132 2.6. Thermal desorption method for Hg speciation

133 The HgTPD device consisted of a thermo-desorption furnace coupled to a PYRO 915 furnace
134 and a continuous mercury analyzer (RA-915) (Rumayor et al., 2015c). The novelty of this device is
135 that in the first furnace the desorption of mercury species is carried out using N₂ as an inert gas to
136 avoid interferences, while at the same time O₂ is introduced into the commercial PYRO furnace to
137 ensure the total decomposition of volatile matter derived from the carbonaceous matter. The sample
138 was weighed in a sample boat and its temperature was controlled by a thermocouple. Measurements
139 were carried out at a heating rate of 50 °C min⁻¹ under a N₂ flow of 500 mL min⁻¹. The PYRO 915
140 unit was kept at 800-1000 °C under an O₂ flow of 500 mL min⁻¹.

141

142 2.6. Characterisation of bauxites

143 The elemental composition of the samples was determined through X-ray fluorescence (XRF)
144 using a PANanalytical – MagiX FAST. Surface area was calculated using the Brunauer-Emmett-
145 Teller (BET) adsorption isotherm, and a Micromeritics ASAP 2020 porosimetry instrument using
146 nitrogen gas at -196°C. Identification of the crystalline mineral matter was performed by X-ray
147 diffraction (XRD) in the range of 2θ=10 °-90°. The diffractograms were obtained using a Bruker
148 D8 Advance diffractometer operating at 40 kV and 40 mA.

149

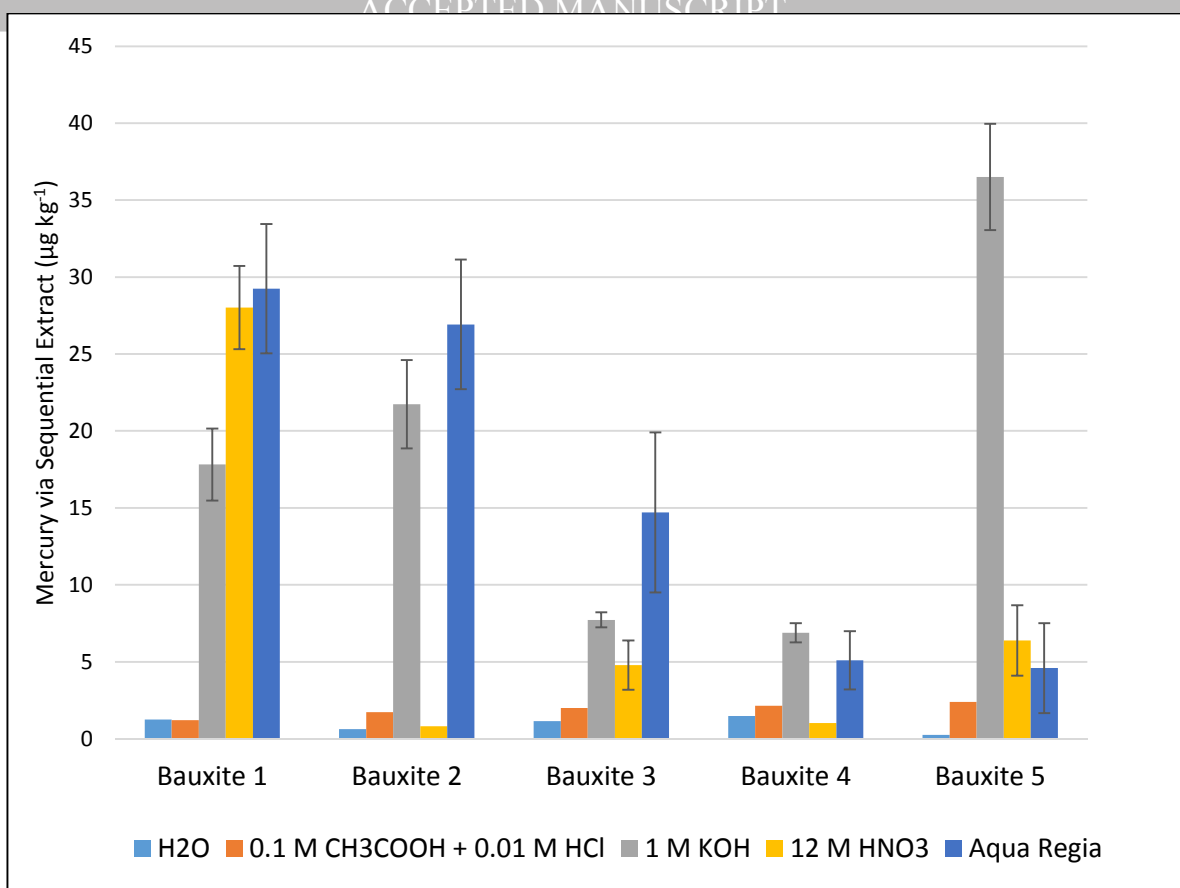
150 3. Results and discussion

151

152 3.1. Sequential extractions

153 The results of the sequential extractions are shown in Figure 1. The sequential extraction results
154 without confidence intervals were below the detection limit of the method. The percent fraction of
155 sequentially extracted mercury is listed in Table 1, with the data below detection limits excluded.
156 The total mercury concentrations determined using hydrofluoric acid total dissolution assay are
157 incorporated into Table 2. No significant amount of mercury was extracted in fraction 1 or 2,
158 suggesting the absence of exchangeable cations and outer sphere adsorbed species. All the bauxites
159 released mercury in fraction 3 (1 M KOH) suggesting that there is an association with organic
160 species. Bauxite 5 is noticeable for releasing the bulk of its sequentially extracted total in fraction 3,
161 and releasing 59 % of its total mercury content in the sequential extraction process, indicating that
162 the mercury in this bauxite is relatively labile (Table 2). However, this lability may be a result of the
163 extremely fine particle size of bauxite 5.

164



165

166 **Figure 1.** Sequential extraction of bauxite (5 replicates).

167

168 **Table 1.** Percent fraction of sequentially extracted mercury (*data below limits of detection omitted*).

	H ₂ O	0.1 M CH ₃ COOH \ 0.01 M HCl	1 M KOH	12 M HNO ₃	Aqua Regia
Bauxite 1	-	-	23.7	37.3	39.0
Bauxite 2	-	-	44.7	-	55.3
Bauxite 3	-	-	28.4	17.6	54.0
Bauxite 4	-	-	57.5	-	42.5
Bauxite 5	-	-	76.9	13.4	9.7

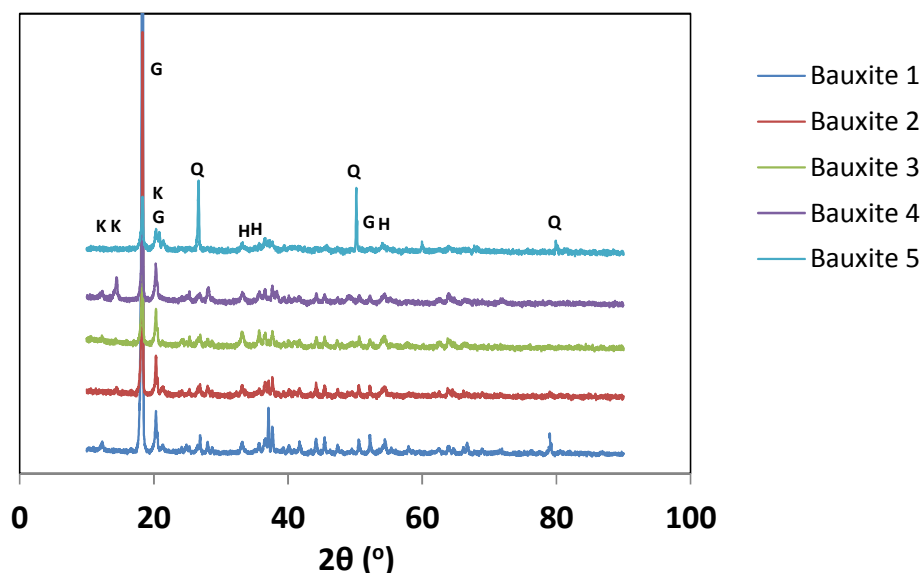
169

170

171 Fraction 4 (12 M HNO₃) is the first fraction which is strongly acidic and oxidising. It is
 172 remarkable that a high proportion of mercury in bauxite 1 was extracted in this fraction, while a
 173 minimal amount of mercury was extracted from bauxite 2. Notionally this implies an absence of

174 elemental mercury in bauxite 2, due to the poor kinetics of cinnabar dissolution in nitric acid, which
175 lacks a strong mercury complexing ligand (Mikac et al., 2003). The redox potential required to
176 preferentially enrich gibbsite and leach iron during bauxitisation is sufficiently reducing to render
177 elemental mercury thermodynamically stable (Petersen, 1971). However, outside of certain
178 hydrothermal deposits and as a minor phase in cinnabar-rich ores, elemental mercury is
179 exceptionally rare (Rytuba, 2003). Hematite, goethite and gibbsite demonstrate substantially
180 increased dissolution kinetics in highly acidic conditions, all of which demonstrates an association
181 with mercury in tropical oxisols (Guedron et al., 2009). In synthetic systems mercury (II) has been
182 found to specifically adsorb to goethite and the gibbsite polymorph bayerite (Collins et al., 1999,
183 Kim et al., 2004), potentially allowing encapsulation to take place during the bauxitisation process,
184 mediated through crystallographic defects. The mercury extracted in fraction 4 may also be
185 indicative of an incomplete extraction of humic acids. It should be noted that sequential extractions
186 at the mercury concentrations analysed here have a poor specificity (Bloom et al., 2003).

187 Pyrite is susceptible to acidic oxidative dissolution (Bryson and Crundwell, 2014). Although
188 the presence of pyrite cannot be ruled out (Figure 2), the fate of mercury-bound pyrite in fraction 4
189 is questionable. If the mercury-sulfur bond remains unbroken, mercury is expected to precipitate as
190 metacinnabar, as sulfide is required to solubilise metacinnabar as a polysulfide aqueous neutral
191 (Clever et al., 1985). Sulfide in nitric acid solutions is rapidly oxidised to elemental sulfur and
192 oxyanionic species (Flatt and Woods, 1995).



193

194 **Figure 2.** XRD analysis of bauxite samples G: Gibbsite; H: Hematite; Q: Quartz; K: Kaolinite

195

196 All the bauxites released significant quantities of mercury in Fraction 5 (aqua regia), indicating
 197 the presence of cinnabar. Bauxites 1, 2 and 3 released most mercury in the strongly acidic and
 198 oxidising fractions, reflecting the relatively refractory nature of the mercury bound in these
 199 bauxites. Bauxites 4 and 5 were comparatively labile. Table 2 lists the sequential extraction sum
 200 total as a percentage of total mercury as determined through total dissolution assay, as well as the
 201 specific surface area determined using the Brunauer–Emmett–Teller (BET) theory. Clearly
 202 sequential extraction dissolves only a small fraction of total mercury. It is worth noting that there is
 203 a loose correlation between lability and surface area, with the exception of bauxite 3. This implies
 204 that a physical process such as solution penetration is governing lability, as the solution must
 205 diffuse through the mineral matrix, which dissolves incompletely at 25°C. As bauxite 3 is a
 206 substantial outlier, it is implied that bauxite 3 contains a significant amount of mercury of a
 207 different chemical speciation, refractory to leaching.

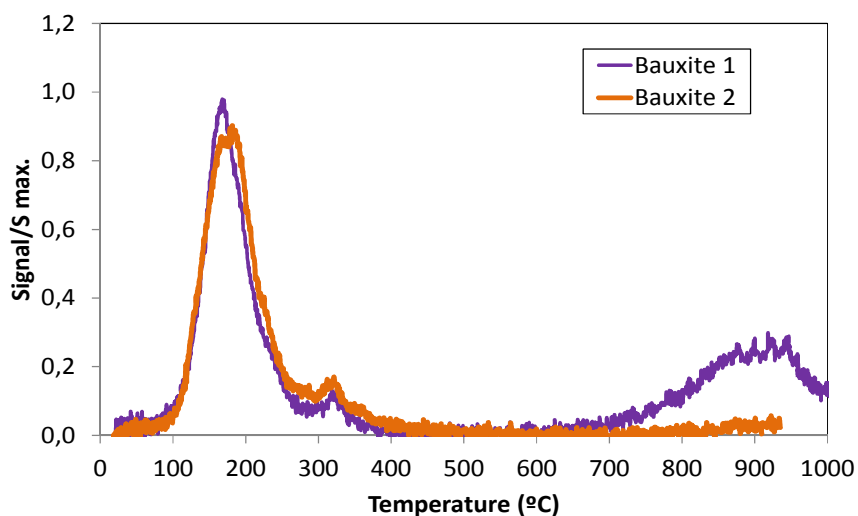
208 **Table 2.** Sum total of sequentially extracted mercury as a percentage of total mercury concentration
 209 and BET surface area (5 replicates).

	Bauxite 1	Bauxite 2	Bauxite 3	Bauxite 4	Bauxite 5
Seq. Extr. Total (ng g⁻¹)	75 ± 9	49 ± 7	27 ± 7	12 ± 3	48 ± 23
HF Total Dissolution (ng g⁻¹)	350 ± 2	218 ± 5	280 ± 3	27 ± 1	82 ± 7
Extraction Efficiency (%)	21	22	10	44	59
BET (m² g⁻¹)	23	44	73	111	126

210

211 3.2. Continuous thermal desorption

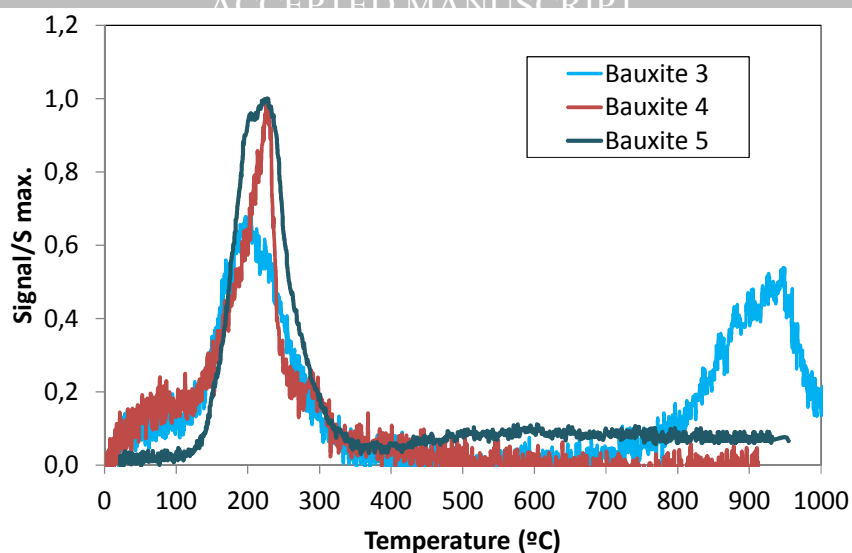
212 The relevant peaks obtained for reference materials are listed in Table 3, including the result of
 213 an unknown iron (III) oxide analysis performed by Reis et al. (2015). HgTPD analysis of all the
 214 bauxites (Figures 3 and 4) show the main band of desorption as being between 125-325 °C.



215

216

217 **Figure 3.** Thermal profiles of bauxite 1 and 2 obtained by means of HgTPD



218

219

220 **Figure 4.** Thermal profile of bauxite 3, 4 and 5 obtained by means of HgTPD

221

222 **Table 3.** HgTPD desorption peaks, as determined by (a) Rumayor et al. (2015c), (b) Reis et al.
223 (2015), (c) Rumayor et al. (2015b) in different species containing mercury

Pyrite (a)	169 °C ± 5
Unknown Iron (III) Oxide (b)	180 °C
Metacinnabar (c)	190 °C ± 11
Humic Acids (c)	220 °C ± 5
Cinnabar (c)	305 °C ± 12
Mercuric Sulfate (c)	583 °C ± 8

224

225 Identification of the species in the low temperature desorption band is difficult. The sequential
226 extraction for bauxite 5 indicate a strong association with organics. However, it has a lower
227 temperature peak which is closer to metacinnabar. The humic acid standard referenced here is acid-
228 soluble by definition and centrifuged to achieve phase separation. Organics in bauxite are a
229 complex assemblage of macromolecular humic substances, and slight changes in temperature peaks
230 are to be expected with varying composition. The varying porosity of the bauxites may also
231 reasonably be expected to affect the desorption kinetics.

232 Cinnabar is the thermodynamically stable mercuric sulfide phase at ambient temperatures, and
233 the desorption data recorded would seemingly eliminate cinnabar as a major mercury sink.
234 However, in soils exposed to mercury contamination in the 1960's, metacinnabar was found to be
235 the predominant phase (Barnett et al., 1997). The organic content in lateritic bauxite is the result of
236 a dynamic process, the leaching and mechanical weathering of soil matter in the surface horizon
237 (Power et al., 2011). The mercury present in surface organics is a product of biogeochemical
238 cycling and is predominantly metacinnabar in the anoxic layer. Moreover, the high binding
239 potential of mercury with sulfur ligands in humic substances favours the mercury-organics
240 association, and organics are known to stabilise metacinnabar in solution (Deonarine and Hsu-Kim,
241 2009, Ravichandran, 2004). Therefore, organics are a source of both mercury and sulfur, and may
242 mobilise metacinnabar to the bauxite horizon. In this case, the low temperature desorption band for
243 all the bauxites may be taken to be indicative of organics and-or metacinnabar.

244 Bauxites 1 and 2 show a small, but definitive, cinnabar peak. It is unlikely that cinnabar exists
245 in the absence of metacinnabar, and the major low temperature peak may be assumed to contain a
246 metacinnabar contribution.

247 Bauxites 1 and 3 show a broad high temperature peak, above 900 °C (Figures 3 and 4). This
248 peak matches no known reference material. The highest desorption temperature recorded is 583 °C
249 for mercuric sulfate (Table 3). Bauxite 3 contains a substantial concentration of this unknown
250 mineral phase, and this chemical difference is the source of its refractory response to sequential
251 extraction. Bloom et al. (2002) demonstrated that a variety of bauxites require temperatures in
252 excess of 900 °C to achieve complete liberation of mercury. To obtain a similar result using an
253 aqueous digestion hydrofluoric acid (HF) was required, reflecting an association with refractory
254 silicates. The inadequacy of aqua regia digestions and the requirement of HF to release all mercury
255 was similarly encountered by Bloom et al. (2002). Gibbsite is highly soluble in strong acids (Dietzel
256 et al., 2005), and kaolinite rapidly decomposes to release metal cations (Carrol & Walther, 1990),

257 leaving quartz and other refractory silicates the mineral phases insoluble in strong acid digestion
 258 without HF.

259 Table 4 compares the total mercury concentrations using hydrofluoric acid total dissolution,
 260 aqua regia digestion and the alkaline digestion method at 140 °C using Bayer liquor. The mercury
 261 content for alkaline digestion was determined by thermal desorption analysis of the residue at 750
 262 °C and a subsequent mass balance. Once extracted to solution, mercury is easily desorbed from the
 263 residue as the elemental species, since digestion conditions are highly reducing (Bansal et al.,
 264 2014b).

265 **Table 4.** Bauxite total mercury concentration as determined by total dissolution, aqua regia
 266 digestion and alkaline digestion methods (5 replicates).

	Bauxite 1	Bauxite 2	Bauxite 3	Bauxite 4
HF Total Dissolution (ng g⁻¹)	350 ± 2	218 ± 5	280 ± 3	27 ± 1
Aqua Regia Digestion (ng g⁻¹)	272 ± 13	226 ± 10	136 ± 9	36 ± 4
Alkaline Digestion (ng g⁻¹)	363 ± 6	224 ± 6	280 ± 3	25 ± 2

267

268 The close correlation of alkaline digestion with the total dissolution results (Table 4) indicates
 269 complete extraction of mercury. This would seemingly indicate that mercury is not associated with
 270 quartz, as alkaline quartz dissolution at 140 °C is insignificant (Oku & Yamada, 1971). Bauxite 3
 271 shows minor quartz peaks in the XRD analysis (Figure 2) and a silica content of 3 % (Table 5).
 272 Furthermore, Figures 3 and 4 clearly demonstrate that high temperature desorption of mercury is
 273 isolated to bauxites 1 and 3. Table 4 demonstrates aqua regia digestion extracted all mercury, except
 274 in the case of bauxites 1 and 3. This refractory mercury was extracted with the addition of HF to the
 275 aqua regia digestion. This is contradictory of the alkaline digestion data, as it strongly implies that
 276 refractory mercury is associated with quartz and other refractory silicates.

277 **Table 5.** Elemental composition as determined by XRF, presented as percentages of oxide

	LOI	Al ₂ O ₃	Fe ₂ O ₃	SO ₃	SiO ₂	TiO ₂
Bauxite 1	28.7	53.9	10.3	0.08	5.3	1.5
Bauxite 2	26.3	48.6	19.9	0.08	2.0	2.7
Bauxite 3	25.5	47.2	21.0	0.06	3.0	2.8
Bauxite 4	24.1	53.2	13.2	0.06	6.5	2.6
Bauxite 5	21.0	39.8	17.0	0.14	20.1	1.3

278

279 The results obtained by HgTPD suggest that the high-temperature release of mercury could be
 280 sulfate-associated (Table 3). This association may develop as sulfide associated mercury is
 281 oxidised. Alunite is a basic potassium aluminium sulfate that is known to be present in bauxite and
 282 undergoes substantial thermal decomposition in excess of 800 °C as the sulfate sublimates
 283 (Foldvari, 2011). However, basic sulfate minerals of similar composition, such as jarosite, are
 284 dissolved easily in aqua regia digestion (Basciano & Peterson, 2008). Table 4 demonstrates that this
 285 does not occur for the refractory mercury in bauxites 1 and 2. Taking into account also that alunite
 286 is a rare mineral in bauxite, alunite is an unlikely candidate.

287 As the complete extraction of mercury using alkaline digestion at 140 °C renders hematite,
 288 goethite, boehmite and quartz as unlikely sources, and sulfidic mercury is proven to desorb at low
 289 temperature, it could be proposed that the mercury is strongly bound to either gibbsite or kaolinite,
 290 both of which are soluble or decompose in alkaline digestion. This implies incorporation into the
 291 mineral lattice as opposed to specific adsorption. Isomorphous and interstitial substitutions are
 292 unlikely. However, in trace concentrations and in the presence of nanoparticulate mesocrystals,
 293 unorthodox reactions can occur, as demonstrated by data suggesting the structural incorporation of
 294 oxidised mercury into growing nanoparticulate goethite (Kim et al., 2007). This proposition of
 295 mercury associated with amphoteric species is contradicted by Table 4, as gibbsite and kaolinite
 296 will dissolve or decompose respectively in aqua regia digestion.

297 Alternatively, it is possible that the bauxitic quartz in this instance is nanocrystalline, has high
 298 surface energy and therefore is susceptible to alkaline digestion at low temperature. A similar
 299 suggestion may be made for feldspars, and both are tectosilicate parent minerals in bauxite.

300 Tremblay et al. (2014) reported that noble gases can be incorporated into quartz and feldspars
301 through their presence in the melt, and elemental mercury shares their neutral, volatile character,
302 and lack of silicate chemical reactivity. Dissanayake and Vincent (1975) proposed the incorporation
303 of mercury into a distortion of the hole in the 12 membered ring of the feldspar framework.
304 Therefore, it is possible that trace mercury concentrations are released in solution through the
305 dissolution of nanocrystalline quartz particles.

306 Laskou et al. (2006) performed an emanation thermal analysis (ETA) of bauxite, whereby
307 recoil energy produced by the spontaneous alpha decay of the radium isotope solution results in the
308 penetration of radon gas. Radon is subsequently released through thermal desorption, with an order
309 of magnitude increase in the radon emanation rate post 900 °C, due to increased structural disorder
310 in the mineral phase. Subsequently the emanation rate declines, due to sintering of the bauxite
311 macrostructure. The effect is very similar to that observed for thermal desorption of bauxitic
312 mercury. ETA analysis of quartz demonstrates a similar increase in kinetics, but without a
313 subsequent decrease in rate due to sintering (Balek et al., 1995). If mercury is transformed by a
314 redox reaction at high temperature, and thermally desorbs as the elemental species and not a
315 charged ionic gas, the kinetics of solid state diffusion then desorption of the elemental gas are likely
316 similar to neutral gases of similar atomic radius such as radon.

317

318 **4. Conclusions**

319 The geochemical speciation of mercury in bauxites was evaluated using sequential extractions,
320 continuous thermal desorption and alkaline digestion methodologies. Sequential extractions
321 indicated the relative lability of bauxitic mercury, and some correlation between lability and
322 specific surface area. All the bauxites showed a main low-temperature band during thermal
323 desorption, indicative of mercury associated with organics or metacinnabar. Bauxites 1 and 2
324 showed a definite cinnabar peak, probably coexistent with metacinnabar. Bauxites 1 and 3 exhibited

325 a very high-temperature desorption peak, associated with refractory bauxitic mercury. The use of
326 thermal desorption and wet chemical methods isolates the unidentified mineral phase to mercury
327 associated with quartz and other refractory silicates.

328

329 **Acknowledgments**

330 Financial support for this research was provided Rio Tinto and by the project GRUPIN14-031.

331

332 **References**

333 Balek, V., Fusek, J., Kříž, J., Murat, M., 1995. Differences in the thermal behaviour of natural
334 quartz before and after mechanical grinding as observed by emanation thermal analysis.
335 *Thermochim. Acta.* 262, 209-214.

336 Bansal, N., Vaughan, J., Boullemant, A., Leong, T., 2014a. Determination of total mercury in
337 bauxite and bauxite residue by flow injection cold vapour atomic absorption spectrometry.
338 *Microchem. J.* 113, 36-41.

339 Bansal, N., Vaughan, J., Tam Wai Yin, P., Leong, T., Boullemant, A., 2014b. Chemical
340 thermodynamics of mercury in the Bayer process. *Hydrometallurgy.* 2, 559 - 569.

341 Barnett, M.O., Harris, L.A., Turner, R.R., Stevenson, R.J., Henson, T.J., Melton, R.C., Hoffman,
342 D.P., 1997. Formation of Mercuric Sulfide in Soil. *Environ. Sci. Technol.* 31, 3037-3043.

343 Basciano, L., Peterson, R., 2008. Crystal chemistry of the natrojarosite-jarosite and natrojarosite-
344 hydronium jarosite solid-solution series: A synthetic study with full Fe site occupancy. *Am.*
345 *Mineral.* 93, 853-862.

346 Bloom, N.S., Vondergeest, V., Preus, E., 2002. Intercomparison of four methods for the
347 determination of total mercury in recalcitrant solids. Annual Meeting of SETAC Europe.
348 Vienna.

- 349 Bloom, N.S., Preus, E., Katon, J., Hiltner, M., 2003. Selective extractions to assess the
350 biogeochemically relevant fractionation of inorganic mercury in sediments and soils. *Anal.*
351 *Chim. Acta.* 479, 233-248.
- 352 Bryson, L.J., Crundwell, F.K., 2014. The anodic dissolution of pyrite (FeS₂) in hydrochloric acid
353 solutions. *Hydrometallurgy.* 143, 42-53.
- 354 Carrol, S., Walther, J., Kaolinite dissolution at 25°C, 60 °C and 80 °C. *Am. J. Sci.* 290, 797-810.
- 355 Clever, L., Johnson, S., Derrick, M., 1985. The solubility of mercury and some sparingly soluble
356 mercury salts in aqueous electrolyte solutions. *J. Phys. Chem. Ref. Data.* 14, 631-680.
- 357 Collins, C.R., Sherman, D.M., Ragnarsdottir, K.V., 1999. Surface complexation of Hg²⁺ on
358 goethite: Mechanism from EXAFS spectroscopy and density functional calculations. *J.*
359 *Colloid Interf. Sci.* 219, 345-350.
- 360 Deonarine, A., Hsu-Kim, H., 2009. Precipitation of mercuric sulfide nanoparticles in NOM-
361 containing water: Implications for the natural environment. *Environ. Sci. Technol.* 43, 2368-
362 2373.
- 363 Dietzel, M., Böhme, G., 2005. The dissolution rates of gibbsite in the presence of chloride, nitrate,
364 silica, sulfate, and citrate in open and closed systems at 20°C. *Geochim. Cosmochim. Acta,*
365 69, 1199-1211.
- 366 Dissanayake, C., Vincent, E., 1975. Mercury in rocks and minerals of the Skaergaard intrusion, East
367 Greenland. *Mineral. Mag.* 4, 33-42.
- 368 Flatt, J.R., Woods, R., 1995. A voltammetric investigation of the oxidation of pyrite in nitric acid
369 solutions: relation to treatment of refractory gold ores. *J. Appl. Electrochem.* 25, 852-856.
- 370 Foldvari, F., 2011. Handbook of thermogravimetric system of minerals and its use in geological
371 practice. *Occasional Papers of the Geological Institute of Hungary,* 213, 1-279.
- 372 Guedron, S., Grangeon, S., Lanson, B., Grimaldi, M., 2009. Mercury speciation in a tropical soil
373 association; Consequence of gold mining on Hg distribution in French Guiana. *Geoderma.*
374 153, 331-346.

- 375 Jew, A.D., Kim, C.S., Rytuba, J.J., Gustin, M.S., Brown, G.E., 2011. New technique for
376 quantification of elemental hg in mine wastes and its implications for mercury evasion into
377 the atmosphere. *Environ. Sci. Technol.* 45, 412-417.
- 378 Kim, C.S., Lentini, C.J., Waychunas, G.A., 2007. Chapter 6 Associations between iron
379 oxyhydroxide nanoparticle growth and metal adsorption/structural incorporation. 7, 153-
380 185.
- 381 Kim, C.S., Rytuba, J.J., Brown, G.E., 2004. EXAFS study of mercury(II) sorption to Fe- and Al-
382 (hydr)oxides. *J. Colloid Interf. Sci.* 271, 1-15.
- 383 Laskou, M., Margomenou-Leonidopoulou, G., Balek, V., 2006. Thermal characterization of bauxite
384 samples. *J. Therm. Anal. Calorim.* 84, 141 –145.
- 385 Mikac, N., Foucher, D., Niessen, S., Lojen, S., Fischer, J.C., 2003. Influence of chloride and
386 sediment matrix on the extractability of HgS (cinnabar and metacinnabar) by nitric acid.
387 *Anal. Bioanal. Chem.* 377, 1196-201.
- 388 Mullett, M., Pendleton, P., Badalyan, A., 2012. Removal of elemental mercury from Bayer stack
389 gases using sulfur-impregnated activated carbons. *Chem. Eng. J.* 211-212, 133-142.
- 390 Mullett, M., Tardio, J., Bhargava, S., Dobbs, C., 2007. Removal of mercury from an alumina
391 refinery aqueous stream. *J. Hazard. Mater.* 144, 274-82.
- 392 Oku, T., Yamada, K., 1971. The dissolution rate of quartz and the rate of desilication in the Bayer
393 process. *Light Metals 1971*. AIME. New York.
- 394 Petersen, U., 1971. Laterite and bauxite formation. *Econ. Geol.* 66, 1070-1071.
- 395 Power, G., Loh, J.S.C., Niemelä, K., 2011. Organic compounds in the processing of lateritic
396 bauxites to alumina: Part 1. *Hydrometallurgy.* 108, 149-151.
- 397 Ravichandran, M., 2004. Interactions between mercury and dissolved organic matter--a review.
398 *Chemosphere.* 55, 319-31.

- 399 Reis, A.T., Coelho, J.P., Rucandio, I., Davidson, C.M., Duarte, A.C., Pereira, E., 2015. Thermo-
400 desorption: A valid tool for mercury speciation in soils and sediments? *Geoderma*. 237-238,
401 98-104.
- 402 Rumayor, M., Diaz-Somoano, M., Lopez-Anton, M.A., Martinez-Tarazona, M.R., 2013. Mercury
403 compounds characterization by thermal desorption. *Talanta*. 114, 318-22.
- 404 Rumayor, M., Diaz-Somoano, M., Lopez-Anton, M.A., Martinez-Tarazona, M.R., 2015a.
405 Application of thermal desorption for the identification of mercury species in solids derived
406 from coal utilization. *Chemosphere*. 119, 459-65.
- 407 Rumayor, M., Fernandez-Miranda, N., Lopez-Anton, M.A., Diaz-Somoano, M., Martinez-
408 Tarazona, M.R., 2015b. Application of mercury temperature programmed desorption
409 (HgTPD) to ascertain mercury/char interactions. *Fuel Process. Technol.* 132, 9-14.
- 410 Rumayor, M., Lopez-Anton, M.A., Díaz-Somoano, M., Martínez-Tarazona, M.R., 2015c. A new
411 approach to mercury speciation in solids using a thermal desorption technique. *Fuel*. 160,
412 525-530.
- 413 Rytuba, J.J., 2003. Mercury from mineral deposits and potential environmental impact. *Environ.*
414 *Geol.* 43, 326-338.
- 415 Staun, C., Vaughan, J., Morrison, H., 2016. Stabilisation of mercury during bayer process digestion.
416 International Mineral Processing Congress. Quebec City, Canada.
- 417 Tremblay, M.M., Shuster, D.L., Balco, G., 2014. Cosmogenic noble gas paleothermometry. *Earth*
418 *and Planetary Science Letters*, 400, 195-205.

419

420

421

422

423 **Figure captions**424 **Figure 1.** Sequential extraction of bauxite (5 replicates).425 **Figure 2.** XRD analysis of bauxite samples G: Gibbsite; H: Hematite; Q: Quartz; K: Kaolinite426 **Figure 3.** Thermal profiles of bauxite 1 and 2 obtained by means of HgTPD427 **Figure 4.** Thermal profile of bauxite 3, 4 and 5 obtained by means of HgTPD

ACCEPTED MANUSCRIPT

- Mercury is present in bauxite at trace concentrations
- Thermal desorption is utilised as a novel technique for mercury geochemical speciation
- Mercury species in bauxite are distinctly refractory or labile to thermal desorption
- Hydrofluoric acid dissolution assay is required to determine total mercury concentration

ACCEPTED MANUSCRIPT